The Cryogenic Fountain ITCsF2

Filippo Levi, Claudio Calosso, Davide Calonico, Luca Lorini, Elio K. Bertacco, and Aldo Godone
Istituto Nazionale di Ricerca Metrologica
Torino, Italy
f.levi@inrim.it

Giovanni A. Costanzo and Barbara Mongino
Politecnico di Torino,
Torino, Italy

Steven R. Jefferts, Thomas P. Heavner and Elizabeth A. Donley
Time and Frequency Division, 847
National Institute of Standards and Technology
Boulder, Colorado, USA

***Abstract*—This paper describes the new twin laser-cooled Cs fountain primary frequency standards NIST-F2 and IT-CsF2, and presents their most innovative design features. Most significant is a cryogenic microwave interrogation region which dramatically reduces the blackbody radiation shift. We present as well a preliminary accuracy evaluation of IT-CsF2.**

I. INTRODUCTION

Since the first calibration of International Atomic Time (TAI) performed with a laser-cooled Cs fountain, the accuracy of this type of standard has improved by nearly a factor of 10 [1, 2]. INRIM and NIST have both contributed to TAI with their fountain IT-CsF1 and NIST-F1. Both fountains have achieved a fractional frequency accuracy in the 10^{-16} range. In typical accuracy evaluation, one of the most important sources of uncertainty in Cs fountains is the blackbody radiation shift (BBRS).

A seminal work of W. Itano [3], explains the equivalence between AC and DC stark shift and from this assumption calculates the BBRS as a function of the radiation temperature of the whole Ramsey interaction region. This work introduces the well known theoretical relation that connects the BBRS to the temperature (1), showing its strong dependence upon the environmental temperature as expected from the Plank Radiation Theory.

$$\frac{\Delta\nu}{\nu_0} = \beta\left(\frac{T}{T_0}\right)^4\left[1+\varepsilon\left(\frac{T}{T_0}\right)^2\right] \qquad (1)$$

Over the past few years several scientific works [4, 5, 6] addressed the absolute value and the related uncertainty of the black body radiation shift bias in Cs primary frequency standards, questioning the level of uncertainty that can be eventually assigned to the shift.

As a matter of fact discrepancies in the experimental value of β are reported in literature [4, 5], and only recent theoretical works [7,8] have presented satisfactory agreement with the value reported in [4] by Simon. On the other hand to attain a BBRS uncertainty capable of pushing the Cs final uncertainty at the level of $1\text{x}10^{-16}$, requires a knowledge of the absolute value of the radiation temperature of fraction of degree at room temperature, task that can be difficult in a large and complex structure like the Ramsey interaction region of a fountain.

The realization of a liquid Nitrogen cooled fountain, together with some care in the design that will be presented in the next paragraphs, allows the reduction of the total BBRS to 1×10^{-16}, with a similar large reduction in its uncertainty. Two of such fountains developed at NIST and INRIM time and frequency laboratories are undergoing preliminary extensive tests.

II. THE CRYOGENIC FOUNTAIN STRUCTURE

The design of the physics package presented here, along with preliminary experimental results, have been previously described in [9,10]. The design of the cryogenic fountain is derived from the original design of NIST-F1 [11], which started operation in 1998, and exhibits a fractional frequency accuracy of 4×10^{-16}. In figure 1 a schematic of the cryogenic fountain is presented. The fountain system is divided in two parts a UHV region and a HV region.

The UHV region includes the trapping and detection vacuum chamber and the Ramsey interaction zone: the vacuum level in this region is in the 10^{-8} Pa. The HV part contains the C-field, two compensation coils, two inner magnetic shields, the cryostat and a third shield. This last component is the only one at room temperature. Despite the number of parts present in this region, cryopumping yields a fairly good vacuum level of 10^{-6} Pa in this region.

978-1-4244-3510-4/09/$25.00 ©2009 IEEE

A. The Ramsey Interaction Zone

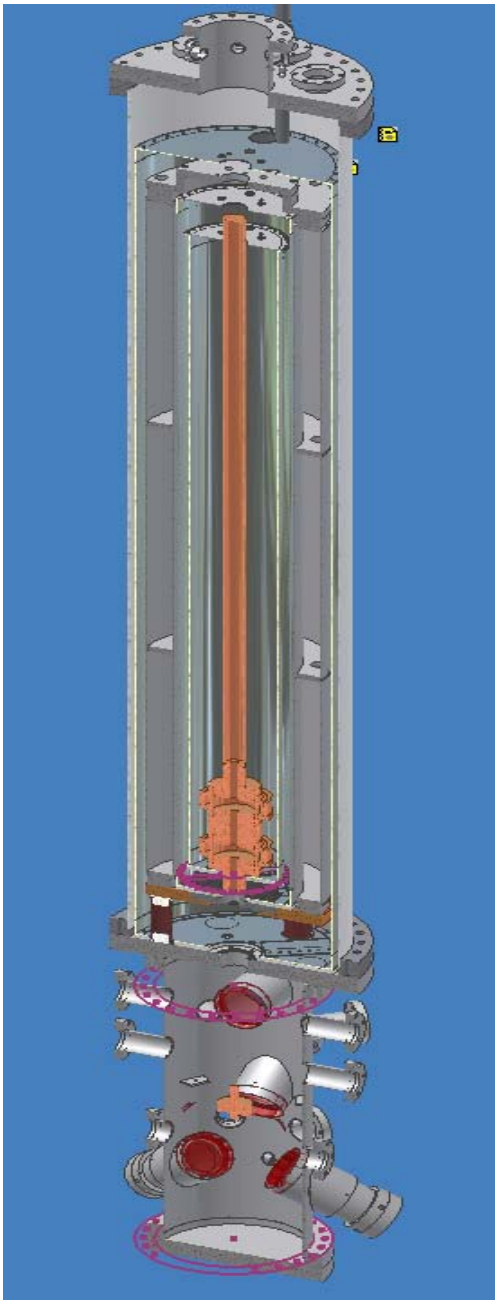

Figure 1. Drawings of the cryogenic fountain.

The Ramsey interaction region is not in a liquid nitrogen bath: the nitrogen is contained in a ~20 l cryostat and the cooling process takes place by conductive and radiative processes. To help this cooling process two endcaps, with good thermal contact are fixed at both end of the cryostat, and the cavity system sits on top of the lower one. In absence of active control, the temperature fluctuates freely according to the amount of liquid nitrogen present in the cryostat. In Figure 2 the temperature profile of the Ramsey interaction zone is shown.

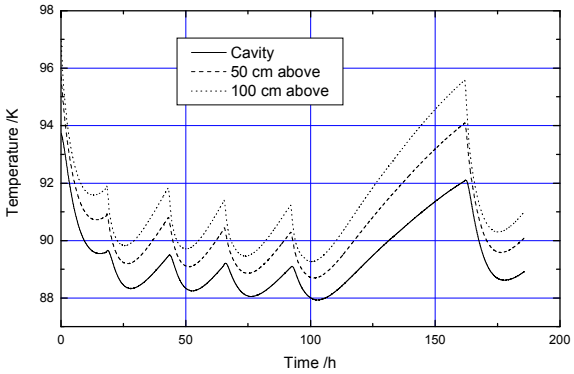

Figure 2. Temperature profile of IT-CsF1 interaction region during one week of operation. The peaks correspond to N_2 fillings of the cryostat.

At room temperature the Ramsey cavity frequency is calculated to be 31 MHz lower than Cs resonance. In the project stage the final temperature of the Cavity was expected to be several degrees below the achieved value, so the cavity was manufactured to be resonant with Cs at 80 K, while the typical temperature of the cavity is around 89 K. This means the Ramsey cavity is detuned almost 1MHz with respect to the atomic resonance. The cavity is thus currently operated out of resonance, but despite the need for higher microwave power, this detuning strongly reduces the sensitivity to phase and power changes due to the temperature oscillations.

Upon cooling the cavity the linewdeith changes from 550 kHz to 250 kHz, in fair agreement with the Gruneisen (2) relation that connects the surface resistivity of the metals to the temperature (predicting a 2.5 ratio); Θ is the Cu Debye temperature.

$$\rho \propto T \cdot \left(\frac{T}{\Theta}\right)^4 \int_0^{\left(\frac{\Theta}{T}\right)} \frac{s^5 ds}{(e^s - 1)(1 - e^{-s})} \qquad (2)$$

The cryogenic part of the fountain contains also the C-field bobbin and two magnetic shields. The magnetic field is generated by a 1.5 m long solenoid that generates a nominal field of 2.5×10^{-4} T/A. Special care was taken during the fountain design in order to avoid the development of thermal currents. However two cylindrical shields are placed in the cryogenic environment. The third magnetic shield instead is still under vacuum but at room temperature. Thermal insulation between the cryostat and the outer shield is provided by several layers of aluminized mylar insulator.

B. The Optical Bench

The fountain is operated in the (1,1,1) geometry to avoid the need of a vertical trapping laser beam. Six independent laser beams are generated by a high power (~ 500 mW) laser source and are amplitude and frequency fine tuned through double pass Acousto-Optic-Modulators (AOM) [12]. The beams are delivered to the cooling region by means of PM

fibers, the total power delivered to the atoms is approximately 15 mW per beam. In order to reduce the laser amplitude noise and to compensate polarization to amplitude noise conversion, active amplitude control of the laser beams is implemented in each AOM branch. For this purpose a beam sampler is placed inside each collimator. In Figure 3 the amplitude noise spectrum at the collimator output is represented in the open and closed loop configuration, together with the noise spectral density of the voltage reference and that of the detector. The post cooling amplitude ramp is also generated by means of this control loop.

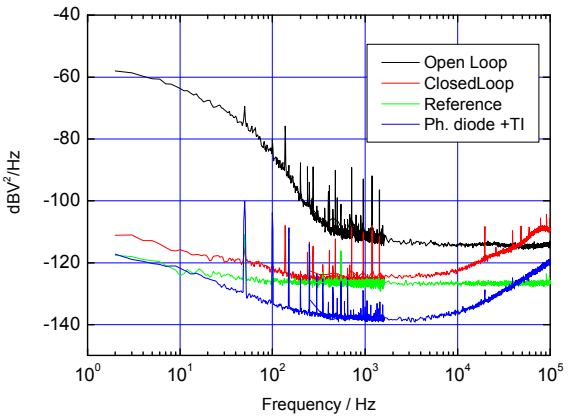

Figure 3. Laser amplitude noise spectrum

The detection beams are generated by independent AOM systems. The repumper beams both for the trap and the detection, are generated by an extended cavity laser.

C. *Atomic Signal and Stability*

In NIST-F2 and IT-CsF2 direct molasses loading in a lin ⊥ lin configuration is implemented. The optical molasses is directly loaded from Cs vapor. No MOT loading nor beam slowing is provided, enough atoms are however collected in order to achieve a shot noise compatible with our LO (BVA oscillator).

Even if a fine tuning of the post cooling process is still required preliminary results have shown already a S/N of 400 in the detected transition probability, allowing for a short term stability $\sigma_y(\tau)= 2.3\times10^{-13}\tau^{-1/2}$. The molasses temperature achieved so far is around 1.5 μK leaving us with an average density shift and a dead time in the duty cycle time a bit higher than our target value.

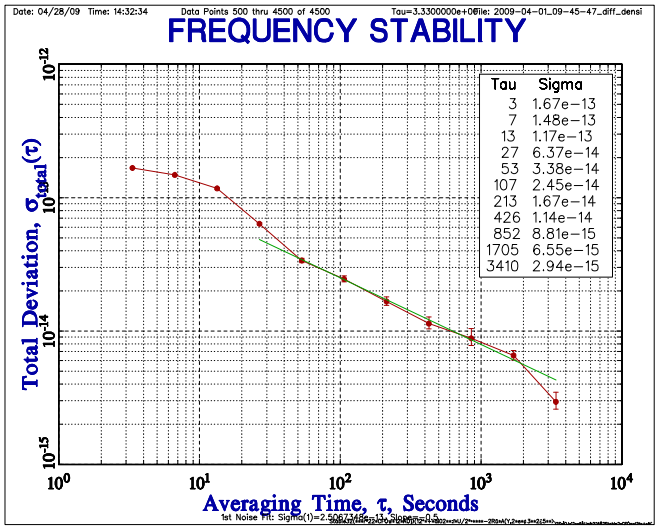

Figure 4. Short term stability of IT Cs-F2

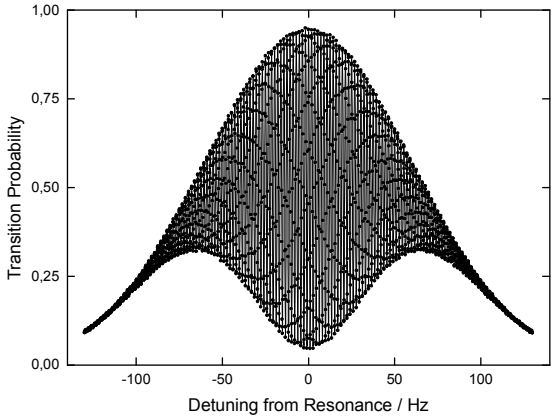

Figure 5. Ramsey fringes of IT Cs-F2

III. Preliminary Accuracy Evaluation

In the following paragraph we report a preliminary accuracy budget for IT-CsF2. The main biases have been evaluated even if the ultimate accuracy of the fountain has not yet been achieved.

A. *Zeeman Effect*

In a similar way to that used in IT-CsF1 and NIST-F1, the C-field is evaluated through the excitation of the low frequency, magnetic sensitive, Majorana transitions between the $|F=3, m_F=0\rangle$ and $|F=3, m_F=\pm1\rangle$ states [13]. To this purpose, a long transversal coil is placed along the whole interaction region. When atoms reach apogee a 100 ms pulse is applied, giving as a result the local value of the magnetic field. The results of the map are used to obtain the time integral value of

Zeeman shift. This calculation predicts the position of the central Ramsey fringe for the magnetic sensitive transition $|F=3, m_F=1\rangle \rightarrow |F=4, m_F=1\rangle$. Since the sampling atomic cloud is not a point-like source, we don't expect a perfect matching of the map with the real field, since a residual spatial/time integration of the field is always present. The discrepancy from the predicted value to the measured one tells us the quality of the map and allows us to determine the uncertainty in the quadratic Zeeman correction we apply to the frequency standard.

In our case the maximum discrepancy observed between the measured value of the central fringe and the calculated one is 100 mHz.

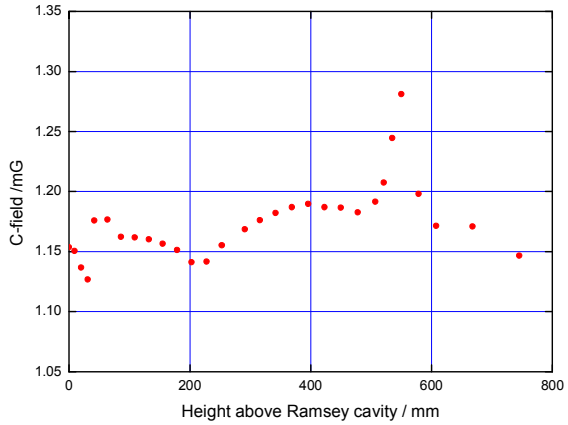

Figure 6. Map of the C field along the interaction region

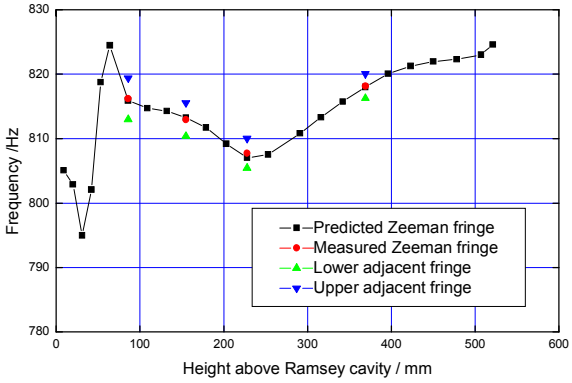

Figure 7. Time integral of the C field, and measurement of the central fringe of the Δm=0, m=-1 transtion

The second source of uncertainty in the Zeeman shift is related to the time stability of the field. We have measured a relative flicker level of the field of 10^{-4}.

Thus, the Zeeman shift and its uncertainty can be written $\frac{\Delta\nu_Z}{\nu} = (633 \pm 0.3)\times 10^{-16}$.

B. Blackbody Radiation Shift

It is extremely difficult to measure with high precision if the radiation temperature of the blackbody corresponds to the temperature measured, especially if the system we are using is not designed to be a blackbody radiator, typically a large spherical cavity with a small hole. In almost all other geometries we have to deal to some extent with reflections at low incidence angle. In F2 we designed the Ramsey interaction region to be as close as we could to a perfect dark body.

There is only one aperture to allow the atoms to go through the cavity (no opening on the top), and the walls of this long channel are threaded in order to avoid low angle reflection. As shown in fig. 2 the temperature is measured with three platinum resistors placed along the interaction region. Given the observed temperature gradient and utilizing the value of β measured in [4] we calculate the BBRS at (90 ±2) K.

$$\frac{\Delta\nu_{BB}}{\nu} = (-1.4 \pm 0.1)\times 10^{-16}$$

C. Microwave Leakage

According to the theory developed in [14] the microwave leakage in F2 can be estimated by means of differential measurements, where the Ramsey excitation amplitude is varied from a π/2 pulse to a (2n-1)π/2 pulse. In these preliminary measurements, we have changed the excitation pulse from π/2 to 3π/2. The results of this procedure extrapolated to π/2 operation are:

$$\frac{\Delta\nu_{Leak}}{\nu} = (7 \pm 8)\times 10^{-16}$$

D. Atomic density shift

The spin exchange shift is typically one of the most relevant biases in Cs fountains. Several techniques have been studied in the last few years in order to reduce or better control this shift [15, 16, 17]. For the moment none of these techniques are implemented in F2, even if the physical structure of the fountain is designed to be modified in order to implement multiple launching. However NIST-F1 [18] has demonstrated that also in standard molasses operation it is possible to achieve a relative uncertainty in the shift measurement well below 1×10^{-16}.

For the moment however, the post cooling process in F2 is not yet optimized and the return-atom fraction is still lower than our target, forcing us to operate at a relatively higher molasses density. A differential measurement, where the atom density is changed by a factor 3 yields to a shift estimation of the fountain operated in the low density regime of :

$$\frac{\Delta \nu_{SE}}{\nu} = (-39 \pm 21) \times 10^{-16}$$

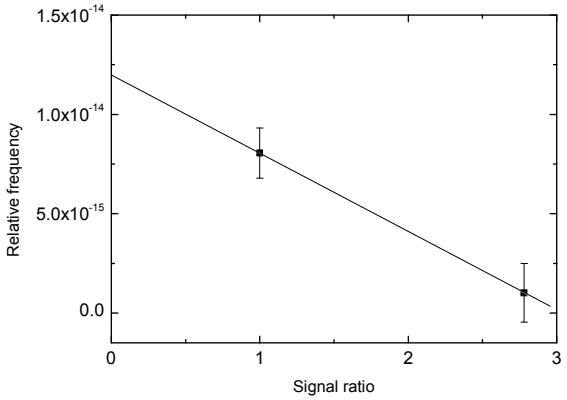

Figure 8. Frequency versus atom density variation

E. Gravitational red shift

The elevation of INRIM on the Geoid was measured recently with high accuracy [19]. The INRIM-F2 elevation is (238.9±0.1)m. The resulting Gravitational red shift is calculated taking into account the value of $\Delta\nu/\nu = 1.09 \times 10^{-16}$/m:

$$\frac{\Delta \nu_{G}}{\nu} = (260.4 \pm 0.1) \times 10^{-16}$$

IV. CONCLUSION

We have presented the physical structure of NIST-F2 and IT-CsF2, two new cryogenically cooled Cs fountain primary frequency standards, developed at NIST (Boulder, USA) and at INRIM (Torino, Italy). We reported as well a preliminary accuracy evaluation of IT-CsF2, showing that no unexpected bias are present at the 10^{-15} level. Further work and investigation will be needed in order to achieve the target accuracy of these two fountains of $\sim 1 \times 10^{-16}$.

REFERENCES

[1] ftp://ftp2.bipm.org/pub/tai/publication/cirt.101

[2] ftp://ftp2.bipm.org/pub/tai/publication/cirt.255

[3] *W. M. Itano, L. L. Lewis and D. J. Wineland, Shift of $^2S_{1/2}$ hyperfine splitting due to blackbody radiation. Phys. Rev. A* ***25****, 1233 (1982).*

[4] *E. Simon, P. Laurent and A. Clairon, Measurement of the Stark shift of the Cs hyperfine splitting in an atomic fountain Phys. Rev. A* ***57****, 436 (1998)*

[5] *F. Levi, D. Calonico, L. Lorini, S. Micalizio, and A. Godone Measurement of the blackbody radiation shift of the 133Cs hyperfine transition in an atomic fountain, Phys. Rev. A* ***70****, 033412 (2004)*

[6] *R Wynands and S Weyers, Atomic fountain clocks* Metrologia ***42*** *No 3 (June 2005) S64-S79*

[7] *E. J. Angstmann, V. A. Dzuba, and V. V. Flambaum, Frequency shift of hyperfine transitions due to blackbody radiation, Phys. Rev. A* ***74****, 023405 2006*

[8] *K. Beloy, U. I. Safronova, and A. Derevianko High-Accuracy Calculation of the Blackbody Radiation Shift in the 133Cs Primary Frequency Standard Phys. Rev. Lett.* ***97****, 040801 (2006)*

[9] *T.P. Heavner, T.E. Parker, J.H. Shirley and S.R. Jefferts, NIST-F1 and F2, Proc. 2008 Symp Freq. Stand. Metrology (in press).*

[10] *S.R. Jefferts, T.P. Heavner, T.E. Parker, J.H.Shirley, NIST Cesium Fountains – Current Status and Future Prospects, Proc. 2007 SPIE conf.*

[11] *S. R. Jefferts et al. Accuracy evaluation of NIST-F1, Metrologia, 2002,* ***39****, 321-336*

[12] *E. A. Donley, T. P. Heavner, F. Levi,M. O. Tataw, and S. R. Jefferts Double-pass acousto-optic modulator system Rev. of Sci. Inst.* ***76****, 063112, 2005*

[13] *F. Levi, L. Lorini, D. Calonico, and A. GodoneIEN-CsF1 Accuracy Evaluation and Two-Way Frequency Comparison IEEE Trans. on UFFC, vol.* ***51****, no. 10, 2004*

[14] *J. H. Shirley, F. Levi, T. P. Heavner, D. Calonico, Dai-Hyuk Yu, and S. R. Jefferts Microwave Leakage-Induced Frequency Shifts in the Primary Frequency Standards NIST-F1 and IEN-CSF1, IEEE Trans on UFFC, vol.* ***53****, no. 12, december 2006*

[15] *F Levi, D Calonico, L Lorini and A Godone IEN-CsF1 primary frequency standardat INRIM: accuracy evaluation and TAI calibrations Metrologia* ***43*** *(2006) 545–555*

[16] *K. Szymaniec, W. Chałupczak, E. Tiesinga, C. J. Williams, S. Weyers, and R. Wynands, Cancellation of the Collisional Frequency Shift in Caesium Fountain Clocks Phys. Rev. Lett.* ***98****, 153002 (2007)*

[17] *F. Pereira Dos Santos, H. Marion, S. Bize, Y. Sortais, A. Clairon, and C. Salomon, Controlling the Cold Collision Shift in High Precision Atomic Interferometry Phys. Rev. Lett.* ***89****, 233004 (2002)*

[18] *T P Heavner, S R Jefferts, E A Donley, J H Shirley and T E Parker NIST-F1: recent improvements andaccuracy evaluations, Metrologia 42 (2005)*

[19] *D Calonico, A Cina, I H Bendea, F Levi, L Lorini1 and A Godone, Gravitational redshift at INRIM Metrologia* ***44*** *(2007) L44–L48*